Extreme Environmental Sensitivity of the Rate of Intramolecular Electron Transfer in Mixed-Valence 1',1'''-Dibenzylbiferrocenium Triiodide

Robert J. Webb,[1] Teng-Yuan Dong,[2] Cortlandt G. Pierpont,[3] Steven R. Boone,[3] Raj K. Chadha,[1] and David N. Hendrickson*,[1]

Contribution from the Department of Chemistry, University of California at San Diego, La Jolla, California 92093-0506, and the Department of Chemistry, University of Colorado, Boulder, Colorado 80309. *Received July 19, 1990*

Abstract: The extreme sensitivity of the rate of intramolecular electron transfer for the mixed-valence 1',1'''-dibenzylbiferrocenium cation to different environments is explored. Two different crystalline morphologies of 1',1'''-dibenzylbiferrocenium triiodide (**1**) could be identified by their different crystal habits (needle and plate-like crystals). They are structurally characterized by single-crystal and powder X-ray diffraction techniques. The single-crystal X-ray structure of a parallelepiped (needle) crystal of **1** at 298 K shows that this polymorph crystallizes in the triclinic space group $P\bar{1}$. The unit cell parameters are a = 9.900 (1) Å, b = 9.962 (1) Å, c = 10.193 (2) Å, α = 112.97 (2)°, β = 114.50 (1)°, and γ = 97.80 (1)° with Z = 1. The structure is also reported for the same crystal at 135 K. An analysis of the full sphere of data again indicates $P\bar{1}$ as the appropriate space group with unit cell constants a = 9.782 (2) Å, b = 9.930 (1) Å, c = 10.108 (2) Å, α = 113.08 (2)°, β = 114.08 (1)°, and γ = 98.06 (1)° with Z = 1. Refinements were carried out with 2990 (6σ) and 3315 (6σ) observed reflections at 298 and 135 K, respectively, to give R = 0.026 and R_w = 0.037 at 298 K and R = 0.025 and R_w = 0.038 at 135 K. Both the mixed-valence 1',1'''-dibenzylbiferrocenium cation and triiodide anion are centrosymmetric at both temperatures. The two crystallographically equivalent metallocene moieties of the cation have dimensions intermediate between those of Fe^{II} and Fe^{III} metallocenes. The packing of **1** consists of weakly interacting 1',1'''-dibenzylbiferrocenium cations forming chains which are surrounded by and separated from other similar chains by the triiodide anions. The 296 K single-crystal X-ray structure of the plate-like crystals of complex **1** show that this polymorph crystallizes in the monoclinic space group $P2_1/n$. The unit cell parameters are a = 22.286 (9) Å, b = 19.413 (10) Å, c = 22.840 (5) Å, and β = 98.55 (3)° with Z = 12. Refinement was carried out with 4486 (6σ) observed reflections to give R = 0.089 and R_w = 0.131. There are three different 1',1'''-dibenzylbiferrocenium cations and three different I_3^- anions in the asymmetric unit. There is not crystallographically imposed symmetry for any of the cations or anions. The temperature dependencies of the ^{57}Fe Mössbauer spectra of the $P\bar{1}$ and $P2_1/n$ polymorphs of complex **1** differ widely. A sample of needle crystallites has a Mössbauer spectrum characteristic of a valence detrapped mixed-valence species down to a temperature of 25 K. On the other hand, a sample of the $P2_1/n$ plate-like crystals exhibits a Mössbauer spectrum characteristic of a valence-trapped species which remains trapped even at 300 K. It was surprising to find that mild grinding of the needle crystallites produces a valence-trapped Mössbauer signal in addition to the valence detrapped signal. Appreciable amounts of the trapped species persist for the ground $P\bar{1}$ needles even up to 300 K. At 7 K, the EPR spectrum of a recrystallized microcrystalline sample of **1** consists of the superposition of three signals: two axial powder patterns each with its own $g_\parallel$ and $g_\perp$ signals and one isotropic g = 2.16 signal. The g tensor anisotropies of the two axial signals are Δg = 1.29 and 0.76. The axial pattern with Δg = 0.76 is assigned to the $P\bar{1}$ form, whereas, the Δg = 1.29 pattern is assigned to the $P2_1/n$ form. The two axial EPR patterns broaden with increasing temperature and the isotropic g = 2 signal gains in relative intensity, so that by 150 K it is the only signal observed. This Lorentzian g = 2.16 signal persists to high temperatures. In contrast, the variable-temperature EPR spectrum of an ethanol glass of **1** shows a single axial signal (Δg = 1.82) which broadens with increasing temperature and becomes unobservable above ~77 K. The EPR properties of mixed-valence 1',1'''-dibenzylbiferrocenium cation are modified by the local environments. Not only does the EPR signal change from the $P\bar{1}$ to the $P2_1/n$ crystal forms but also there is even a sample history dependence of the g values for the two crystal forms. The g = 2.16 signal is the result of *inter*molecular interactions.

Introduction

The rate of electron transfer in chemical and biological systems can be sensitively controlled by environmental factors. In the case of outer-sphere electron transfer between metal complexes in solution, various factors associated with the environment about the donor–acceptor precursor complex may affect the rate.[4] Sluggish solvent molecule motion may be important. There are several cases known[4a] where changes in the anion (cation) in the solution affect the rate of electron transfer between two cationic (anionic) metal complexes. In the case of the $Fe(CN)_6^{3-}/Fe(CN)_6^{4-}$ electron exchange, for example, a change in the cation in solution can dramatically affect the rate of electron transfer.[4b,c] The cation could serve as a bridge between the two anionic complexes in the precursor complex. Perhaps the cation is aggregated with the two anions or it simply changes the ionic strength of the medium. "Environmental" control of rates of electron transfer in biological systems will likely prove difficult to understand.[5] It is clear that the rate of electron transfer between various electron transport proteins is appreciably restrained.[5a] That is, the protein–protein electron-transfer rates are not at all as fast as they can be. The biological design principle has been one of specificity. Protein conformational changes, the onset of motion of internal amino acid residues, reorganization energies, and the dynamics of protein–protein interfaces have been suggested as providing control and specificity in electron transfer between proteins.[5] Furthermore, electron-transfer steps control many important metalloenzyme-catalyzed reactions, such as O_2 reduction to give H_2O in cytochrome-c oxidase[6] and camphor oxidation by

(1) University of California, San Diego.
(2) Present address: Institute of Chemistry, Academia Sinica, Nankang, Taipei, Taiwan.
(3) University of Colorado.
(4) (a) Cannon, R. D. *Electron Transfer Reactions*; Butterworths: London, 1980. (b) Campion, R. J.; Deck, C. F.; King, P.; Wahl, A. C. *Inorg. Chem.* **1967**, *6*, 672. (c) Shporer, M.; Ron, G.; Lowenstein, A.; Navon, G. *Inorg. Chem.* **1965**, *4*, 361. (d) Haim, A. *Comments Inorg. Chem.* **1985**, *4*, 113–149. (e) Jortner, J.; Bixon, M. *J. Chem. Phys.* **1988**, *88*, 167.
(5) (a) Williams, G.; Moore, G. R.; Williams, R. J. P. *Comments Inorg. Chem.* **1985**, *4*, 55. (b) McLendon, G. *Acc. Chem. Res.* **1988**, *21*, 160. (c) Mayo, S. L.; Ellis, W. R., Jr.; Crutchley, R. J.; Gray, H. B. *Science* **1986**, 948. (d) Hoffman, B. M.; Ratner, M. A. *J. Am. Chem. Soc.* **1987**, *109*, 6237.
(6) (a) Bersuker, I. B. *The Jahn–Teller Effect and Vibronic Interactions in Modern Chemistry*; Plenum Press: New York, 1984. (b) Wong, K. Y.; Schatz, P. N. *Prog. Inorg. Chem.* **1981**, *28*, 369.

0002-7863/91/1513-4806$02.50/0

the P-450$_{cam}$ electron-transfer chain.[7]

Studies of electron transfer in mixed-valence transition-metal complexes have revealed that the environment surrounding a mixed-valence molecule is the most important factor in determining the rate of intramolecular electron transfer. The lowest energy electronic states are vibronic, and as a result mixed-valence complexes can be very sensitive to their environments.[6] The most prominent and best characterized examples of the environmental control of intramolecular electron-transfer rates are found in the case of the mixed-valence trinuclear iron acetate complexes,[7] where the onset of ligand motion or solvate molecule dynamics in the solid state triggers a dramatic increase in the electron-transfer rate. The environmental dynamics and the electron-transfer process are coupled.

Several other observations suggest the importance of environmental factors in controlling the rate of intramolecular electron transfer. For instance, it has been reported that aggregation of anions with a cationic mixed-valence complex in solution can affect the near IR intervalence transfer (IT) electronic absorption band and, presumably, the rate of intramolecular electron transfer.[8] The association of the anion with the cation undoubtedly alters the potential energy surface of the mixed-valence molecule, and this affects the electron-transfer rate. Very recently, it has been found that changing the counter anion in disubstituted mixed-valence biferrocenium salts leads to dramatic changes in the electron-transfer rate in the solid state.[9,10] It has been suggested that changing the anion alters the local solid-state environment of the mixed-valence biferrocenium cation and this affects the intracation electron-transfer process. The environmental perturbations caused by changing the anion from I_3^- to PF_6^-, for example, are many and varied. The size, shape, and charge distribution of the two anions are completely different, and all of these factors can ultimately affect the solid-state arrangement adopted by a particular system. One packing of anions about a mixed-valence cation may valence trap the cation. Another packing may turn on electron transfer. It is even likely that the onset of motion associated with an anion such as PF_6^- could increase the rate of electron transfer in a mixed-valence cation.

It has been reported in a preliminary fashion that the spectral properties of 1',1'''-dibenzylbiferrocenium triiodide, **1**, are sample history dependent.[11] It was intriguing to us to find the origins of this sample history dependency. In this paper we report that there is an *extreme* environmental sensitivity of the rate of intermolecular electron transfer in mixed-valence 1',1'''-dibenzylbiferrocenium triiodide. It is shown that intramolecular electron transfer in 1',1'''-dibenzylbiferrocenium triiodide is sensitive to the environmental perturbation caused by differences in crystal packing arrangements. Two polymorphs of **1** have been found, one that is valence trapped up to 300 K and the other which is detrapped down to 25 K. An extreme sensitivity to defect concentration is also reported.

Experimental Section

Compound Preparation. 1',1'''-Dibenzylbiferrocene was synthesized according to literature methods[12] and identified by melting point, ^{1}H NMR, and mass spectral data. 1',1'''-Dibenzylbiferrocenium triiodide, **1**, was synthesized by adding a stoichiometric amount of iodine (172 mg, 0.681 mmol) dissolved in benzene (25 mL) to a benzene solution (25 mL) of 1',1'''-dibenzylbiferrocene (250 mg, 0.454 mmol). The dark blue/black microcrystals that precipitated out of the benzene solution were collected by filtration, washed successively with benzene and diethyl ether, and then dried overnight in a desiccator over Drierite. Anal. Calcd for microcrystalline sample of 1',1'''-dibenzylbiferrocenium triiodide ($C_{34}H_{30}Fe_2I_3$): C, 43.86; H, 3.25; Fe, 12.00. Found: C, 44.36; H, 3.29; Fe, 12.04.

Approximately one-half of the sample (150 mg) prepared in the above manner was recrystallized by dissolving the 1',1'''-dibenzylbiferrocenium triiodide in 100 mL of dichloromethane; then an equal amount of hexane was added. The resulting solution was concentrated by mild heating (T < 50 °C) to approximately one-half the total combined volume. Crystals of 1',1'''-dibenzylbiferrocenium triiodide precipitated from the largely hexane solution upon cooling. Two distinct crystallite morphologies were apparent in the recrystallized microcrystalline sample: needle and plate-like crystals. The sample of mixed crystallites that formed were collected by filtration, washed with diethyl ether, and dried in a desiccator. The crystal morphologies were easily separated under a polarizing microscope into two samples. Microanalyses of the two samples were identical within experimental error. Anal. Calcd for the recrystallized samples of 1',1'''-dibenzylbiferrocenium triiodide ($C_{34}H_{30}Fe_2I_3$): C, 43.86; H, 3.25; Fe, 12.00. Found: C, 42.86; H, 3.24; Fe, 11.86. For a collection of plate crystals we found C, 43.83; H, 3.29; Fe, 11.94.

Physical Methods. ^{57}Fe Mössbauer measurements were made on a constant velocity instrument which has been previously described.[13] The absolute temperature accuracy is estimated to be ±3 K, while the relative precision is ±0.5 K. Mössbauer spectra were least-squares fit to Lorentzian line shapes by means of a computer program described elsewhere.[14]

Isomer shifts are reported relative to iron foil at 300 K but are uncorrected for temperature-dependent, second-order Doppler effects.

Variable-temperature X-band EPR spectra were recorded on a computer-controlled Bruker ER220D-SRC spectrometer equipped with an Air Products digital temperature controller, a Varian gauss meter, and an EPI 548H frequency meter.

The powder X-ray diffraction patterns were recorded at room temperature on a Phillips APD 3600 diffractometer, equipped with a copper X-ray tube (Cu Kα = 1.5406 Å) and graphite monochromator. The powder patterns reported are the result of a single scan from 2θ = 5–30° at 2° per minute on loosely packed polycrystalline samples.

X-ray Structure Determination of 1',1'''-Dibenzylbiferrocenium Triiodide. Dark blue/black parallelepiped crystals of **1** form when a layer of hexane is allowed to slowly diffuse into a concentrated dichloromethane solution of 1',1'''-dibenzylbiferrocenium triiodide, **1**. A crystal of the complex suitable for crystallographic investigation was mounted and aligned on a Nicolet P3F automated diffractometer equipped with a Nicolet LT-2 cryostat for data collection at low temperature. Data were collected on the crystal at ambient temperature and 135 K. Statistical tests indicated that the unit cell was centrosymmetric at both temperatures, and the two redundant hemispheres of data were averaged with values for R_{int} of 0.021 (298 K) and 0.011 (135 K). Both structures determinations were carried out with the SHELXTL library of computer programs. Table I summarizes the crystal data and details of data collection and structure refinement of **1** at 135 and 298 K. Since the structural results obtained at both temperatures are essentially the same and since the refinement of 135 K data is of slightly higher quality, only the results obtained with the low-temperature data will be described in detail. All of the pertinent information concerning the 298 K structure is included in the supplementary material.

The 298 K structure was solved first, and then these results were used as a starting point for the low-temperature structure refinement. The position of the iron and iodine atoms were deduced from an E-map. A subsequent least-squares difference Fourier map indicated the carbon atom positions. The refinement of the 298 K data was conducted with

(7) (a) Jang, H. G.; Geib, S. J.; Kaneko, Y.; Nakano, M.; Sorai, M.; Rheingold, A. L.; Montez, B.; Hendrickson, D. N. *J. Am. Chem. Soc.* **1989**, *111*, 173. (b) Kaneko, Y.; Nakano, M.; Sorai, M.; Jang, H. G.; Hendrickson, D. N. *Inorg. Chem.* **1989**, *28*, 1067. (c) Oh, S. M.; Wilson, S. R.; Hendrickson, D. N.; Woehler, S. E.; Wittebort, R. J.; Inniss, D.; Strouse, C. E. *J. Am. Chem. Soc.* **1987**, *109*, 1073. (d) Woehler, S. E.; Wittebort, R. J.; Oh, S. M.; Kambara, T.; Hendrickson, D. N.; Inniss, D.; Strouse, C. E. *J. Am. Chem. Soc.* **1987**, *109*, 1063. (e) Woehler, S. E.; Wittebort, R. J.; Oh, S. M.; Hendrickson, D. N.; Inniss, D.; Strouse, C. E. *J. Am. Chem. Soc.* **1986**, *108*, 2938. (f) Hendrickson, D. N.; Oh, S. M.; Dong, T.-Y.; Kambara, T.; Cohn, M. J.; Moore, M. F. *Comments Inorg. Chem.* **1985**, *4*, 329. (g) Sorai, M.; Kaji, K.; Hendrickson, D. N.; Oh, S. M. *J. Am. Chem. Soc.* **1986**, *108*, 702. (h) Cannon, R. D.; White, R. P. *Prog. Inorg. Chem.* **1988**, *36*, 195–298.

(8) (a) Hammack, W. S.; Drickamer, H. G.; Lowery, M. D.; Hendrickson, D. N. *Inorg. Chem.* **1988**, *27*, 1307. (b) Hammack, W. S.; Lowery, M. D.; Hendrickson, D. N.; Drickamer, H. G. *J. Phys. Chem.* **1988**, *92*, 1771. (c) Sinha, U.; Lowery, M. D.; Ley, W. W.; Drickamer, H. G.; Hendrickson, D. N. *J. Am. Chem. Soc.* **1988**, *110*, 2471. (d) Sinha, U.; Lowery, M. D.; Hammack, W. S.; Hendrickson, D. N.; Drickamer, H. G. *J. Am. Chem. Soc.* **1987**, *109*, 7340.

(9) (a) Webb, R. J.; Geib, S. J.; Staley, D. L.; Rheingold, A. L.; Hendrickson, D. N. *J. Am. Chem. Soc.* **1990**, *112*, 5031. (b) Webb, R. J.; Rheingold, A. L.; Geib, S. J.; Staley, D. L.; Hendrickson, D. N. *Angew. Chem., Int. Ed. Engl.* **1989**, *28*, 1388.

(10) (a) Dong, T.-Y.; Kambara, T.; Hendrickson, D. N. *J. Am. Chem. Soc.* **1986**, *108*, 5857. (b) Dong, T.-Y.; Kambara, T.; Hendrickson, D. N. *J. Am. Chem. Soc.* **1986**, *108*, 4423.

(11) Dong, T.-Y.; Hendrickson, D. N.; Iwai, K.; Cohn, M. J.; Cohn, S. J.; Rheingold, A. L.; Sano, H.; Motoyama, I.; Nakashima, S. *J. Am. Chem. Soc.* **1985**, *107*, 7996.

(12) Yamakawa, K.; Hisetome, M.; Sako, Y.; Ichida, S. *J. Organomet. Chem.* **1975**, *93*, 219.

(13) Cohen, M. J.; Timken, M. D.; Hendrickson, D. N. *J. Am. Chem. Soc.* **1984**, *106*, 6683.

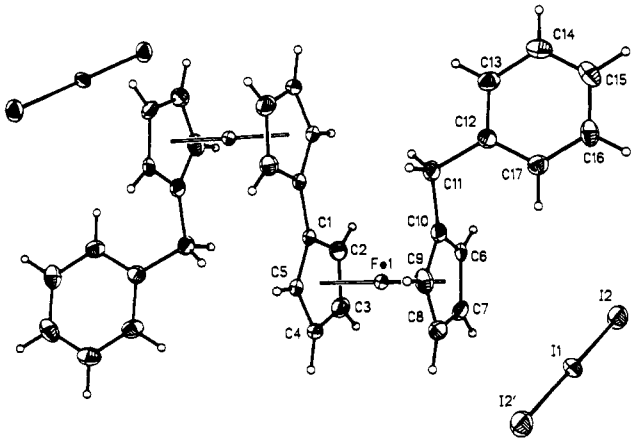

Figure 1. ORTEP drawing for the $P\bar{1}$ polymorphic form of 1′,1‴-dibenzylbiferrocenium triiodide (**1**) at 135 K depicting 30% probability ellipsoids. Inversion symmetry is present for both the cation and the anion.

anisotropic thermal parameters for all non-hydrogen atoms. Hydrogen atoms were included as fixed contributors at ideal distances. Inversion symmetry, imposed on both the cation and the anion, appeared appropriate from an analysis of the full sphere of data and from structural features present. Refinement of the 135 K data set using the atomic positions obtained from the room-temperature refinement revealed slight shifts in atom positions however, none of them were viewed as significant. Final positional parameters and equivalent isotropic thermal parameters for the 135 K $P\bar{1}$ structure of **1** are available in the supplementary material. Table II lists the bond distances and angles for the 135 K structure. Tables of the anisotropic thermal parameters, calculated hydrogen atom positions, and structure factor tables for the 135 K structure are available as supplementary material.

Plate-like crystals of 1′,1‴-dibenzylbiferrocenium triiodide form when a 1:1 dichloromethane/hexane solution was allowed to evaporate slowly. The majority of these crystals were found to diffract poorly, because they all were wafer thin. After careful examination, one crystal was found which had acceptable thickness, although this crystal had an inseparable satellite crystal attached to it. Since this crystal diffracted reasonably well, it was decided to collect data on this crystal. The crystal was mounted on a glass fiber along the longest dimension, and the unit cell dimensions were obtained from 30 reflections in the range $15 < 2\theta < 30°$. Intensities of three monitor reflections measured after every 100 reflections did not show any significant decay. A face-indexed analytical absorption correction was applied to the data, in addition to Lorentz and polarization corrections.

The positions of the I and Fe atoms were obtained by direct methods, and the positions of all carbon atoms were obtained from difference maps. The structure was refined with the SHELXTL programs. The I and Fe atoms were refined anisotropically, while the C atoms were refined isotropically. Hydrogen atoms were not included in the calculations. The maximum height of 1.83 e Å^{-3} in the final ΔF map indicates an ineffective absorption correction. However, the quality of the data preclude further improvements of the results. In Table II are summarized all of the crystal, collection, and refinement data in the $P2_1/n$ polymorph of 1′,1‴-dibenzylbiferrocenium triiodide. Final positional parameters, tables of anisotropic and isotropic thermal parameters, and structure factor tables for the $P2_1/n$ structure of complex **1** are available as supplementary material. In Table III are given selected bond distances and angles for this structure.

Results and Discussion

Single-Crystal X-ray Structures of 1′,1‴-Dibenzylbiferrocenium Triiodide, 1. 1′,1‴-Dibenzylbiferrocenium triiodide exhibits two polymorphic phases at room temperature. The two crystal morphologies are easily distinguishable; one polymorph crystallizes as parallelepipeds (needles), while the other crystallizes as plate-like wafers. Single-crystal structure determinations of the triclinic form of 1′,1‴-dibenzylbiferrocenium triiodide, **1**, were conducted at both 298 and 135 K (Table I). An ORTEP plot of the 1′,1‴-dibenzylbiferrocenium cation and the triiodide anion at 135 K are given in Figure 1, whereas Figure 2 shows a stereoview of the extended packing arrangement adopted in this polymorph. Collected in Table I are selected bond distances and angles for the 135 K structure determination.

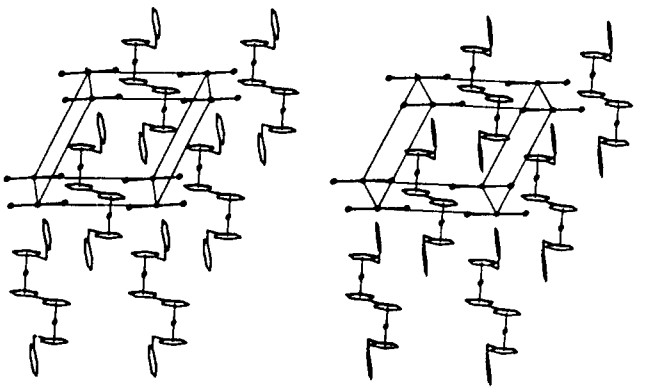

Figure 2. Stereoview of the packing of the $P\bar{1}$ polymorph of 1′,1‴-dibenzylbiferrocenium triiodide (**1**) at 135 K.

The full spheres of data collected on the parallelepiped crystal of **1** at 298 and 135 K indicate $P\bar{1}$ as the choice of space group in both instances. The refinement of the structure imposed inversion centers on both the disubstituted biferrocenium cation as well as the triiodide anion. Comparison of the refined atomic positions for the two structures shows only minor shifts, none of which are significant. The anisotropic thermal parameter, U_{ij}, of all the atoms decreased by approximately one-half upon going from 298 to 135 K. On the basis of these results, the two structures are judged to be identical with the limit of crystallographic resolution. The inversion symmetry of the cation and anion is present at both temperatures.

As shown in Figure 1, the dibenzylbiferrocenium cation adopts the usual trans conformation seen in other mixed-valence disubstituted biferrocenium salts.[11,15-17] Inspection of the iron to cyclopentadienyl ligand bond lengths (Fe–Cp) show that both distances (1.676 and 1.679 Å) are intermediate between the analogous values for neutral ferrocene (1.65 Å)[18] and the ferrocenium ion (1.70 Å).[19] The dihedral angle between the least-squares planes of the Cp rings is 2.3°, while the centroid–Fe–centroid angle is 178.8. The Cp···Cp separation is 3.354 Å with an average Fe–C bond length of 2.070 Å. The two Cp ligands bonded to each iron ion are not perfectly eclipsed but are rotated relative to one another by 6.6°.

The triiodide anion sits on a center of inversion in the unit cell. The I1–I2 bond length is 2.906 Å which compares well with other determinations of the symmetric triiodide bond length.[15-17] The triiodide is strictly linear as required by the inversion symmetry. The anisotropic thermal parameters of the iodine atoms indicate that the motion with greatest amplitude is consistent with a bending vibrational mode rather than an elongation–contraction vibrational mode.

The extended packing of the $P\bar{1}$ polymorph of **1** consists of linear strands of weakly interacting 1′,1‴-dibenzylbiferrocenium cations surrounded by and separated from other similar stands by triiodide anions (Figure 2). The closest cation–cation contacts result from intermolecular contacts of benzyl substituents. However, the benzene rings are not anywhere close to being parallel to each other. Instead they interact in a more perpendicular fashion such that the shortest cation–cation contact (3.05 Å) is associated with the interaction of a hydrogen bonded to ring carbon C9 of a benzyl

(14) Chrisman, B. L.; Tumolillo, T. A. *Comput. Phys. Commun.* **1971**, *2*, 322.
(15) (a) Geib, S. J.; Rheingold, A. L.; Dong, T.-Y.; Hendrickson, D. N. *J. Organomet. Chem.* **1986**, *312*, 241. (b) Dong, T.-Y.; Hendrickson, D. N.; Pierpont, C. G.; Moore, M. F. *J. Am. Chem. Soc.* **1986**, *108*, 963. (c) Cohn, M. J.; Dong, T.-Y.; Hendrickson, D. N.; Geib, S. J.; Rheingold, A. L. *J. Chem. Soc., Chem. Commun.* **1985**, 1095. (d) Dong, T.-Y.; Cohn, M. J.; Hendrickson, D. N.; Pierpont, C. G. *J. Am. Chem. Soc.* **1985**, *107*, 4777.
(16) Lowery, M. D. Ph.D. Thesis, University of Illinois, 1989.
(17) (a) Konno, M.; Sano, H. *Bull. Chem. Soc. Jpn.* **1988**, *61*, 1455. (b) Konno, M.; Hyodo, S.; Iijima, S. *Bull. Chem. Soc. Jpn.* **1982**, *55*, 2327.
(18) Seiler, P.; Dunitz, J. D. *Acta Crystallogr. Sect. B* **1979**, *35*, 1068.
(19) Mammano, N. J.; Zalkin, A.; Landers, A.; Rheingold, A. L. *Inorg. Chem.* **1977**, *16*, 297.

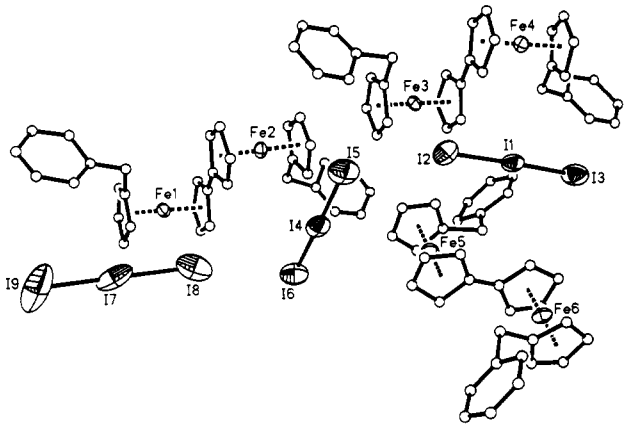

Figure 3. ORTEP drawing showing the three different cations and anions in the 296 K X-ray structure of the $P2_1/n$ polymorph of 1',1'''-dibenzylbiferrocenium triiodide. The atoms are drawn with 30% probability ellipsoids, and the hydrogen atoms are omitted for clarity.

substituent on one cation and C14 of a benzyl substituent on another cation. The triiodide anions sit roughly perpendicular to the cation stacking direction filling the voids in each stack as well as those between stacks. The closest cation–anion contact (3.45 Å) occurs between I2 and the hydrogen atom bonded to C17.

The X-ray structure of the plate-like polymorph of complex **1** shows that it is $P2_1/n$ at 296 K. As shown in Figure 3, there are three $[Fe_2C_{34}H_{30}^+]I_3^-$ molecules in the asymmetric unit. All I_3^- are essentially linear with the average I–I distance of 2.92 (3) Å and average I–I–I angle of 176 (2)°. In contrast to the $P\bar{1}$ polymorph, there is no crystallographic symmetry imposed on any of the three different biferrocenium cations. The average iron to the center of cyclopentadienyl ring distance is 1.663 Å, while the average ring centroid–Fe–centroid angle is 177.2°. The dihedral angle between the least-squares planes of the Cp rings average to 4.5° for cation 1, 6.6° for cation 2, and 4.2° for cation 3. The dihedral angles between the two phenyl rings in the three independent cations of the asymmetric unit are 11.9°, 3.4°, and 8.1°, respectively. A packing diagram is available in the supplementary material.

Powder X-ray Diffraction. Powder X-ray diffraction patterns were collected on samples of the two polymorphs of 1',1'''-dibenzylbiferrocenium triiodide, **1**, and are shown in a figure available in the supplementary material. Comparison of the powder patterns for the plates and the needles clearly indicates that these two different crystal morphologies do indeed represent different crystal packing arrangements for **1** at room temperature. This is in agreement with the single-crystal structural results. Though grinding a sample of needle crystals of **1** does indeed alter its spectroscopic properties (vide infra), it has little effect on the diffraction properties of the sample, as found from the powder diffraction pattern of a ground sample of needles of **1**. The peaks are noticeably broadened, and the overall pattern intensity is decreased. However, grinding does not cause an interconversion between the two characterized crystalline phases. The sole effect of grinding is probably to increase the concentration of defect sites in the crystallites.

^{57}Fe Mössbauer Spectroscopy. It has been reported[11] that the ^{57}Fe Mössbauer spectral properties of 1',1'''-dibenzylbiferrocenium triiodide, **1**, are dependent upon sample history. To examine this phenomenon more thoroughly we prepared samples of **1** by a variety of means. A microcrystalline sample of **1** was prepared by the dropwise addition of an iodine/benzene solution to a benzene solution of 1',1'''-dibenzylbiferrocene. The ^{57}Fe Mössbauer spectrum of this sample at two temperatures, shown in Figure 4A, consists of a valence-trapped (Fe^{II}, $\Delta E_Q \sim 2.0$ mm/s; Fe^{III}, $\Delta E_Q \sim 0.5$ mm/s) and a valence-detrapped ($Fe^{II/III}$, $\Delta E_Q \sim 1.1$ mm/s) signal. Examination of this sample under a polarizing microscope revealed that it was composed of two distinct crystalline morphologies: plate-like and needle microcrystals. A portion of the initial sample was recrystallized in a mixture of hexane and dichloromethane. The recrystallized sample, composed of substantially larger crystallites, consisted mainly of parallelepipeds (i.e., larger versions of the microcrystalline needles). Nevertheless, wafer thin plates were also present. The different morphologies were easily separated into two samples. The ^{57}Fe Mössbauer spectra (at 150 and 300 K) of the parallelepipeds and plate-like crystals are shown in Figure 4 (parts B and C, respectively). The parallelepiped crystalline sample exhibits a spectrum characteristic of valence-detrapped species (150–300 K), while the collection of plate-like crystals gives a valence-trapped spectrum at both temperatures. The Lorentzian line shape fitting parameters for all the spectra displayed in Figure 4 are given in Table IV.

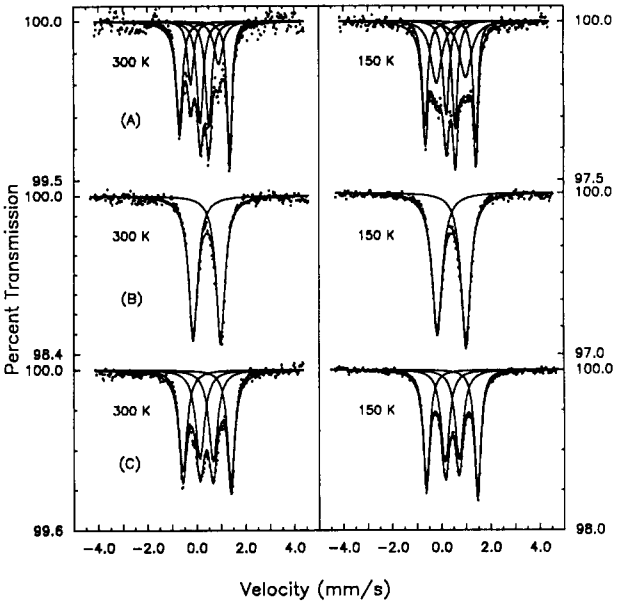

Figure 4. Variable-temperature ^{57}Fe Mössbauer spectrum for various polycrystalline samples of 1',1'''-dibenzylbiferrocenium triiodide (**1**): (A) initial precipitate, (B) needle crystallites, and (C) plate-like crystallites.

It has been shown that ^{57}Fe Mössbauer spectroscopy can be used to monitor the intramolecular electron-transfer rate in mixed-valence biferrocenium salts.[9-11,15-17,20] When the intracation electron-transfer rate is slower than about $\sim 10^6$ s^{-1}, discrete iron valences are sensed by the Mössbauer technique; spectra consist of a superposition of two quadrupole-split doublets with characteristics typical of Fe^{II} and Fe^{III} metallocenes. When the rate of intramolecular electron-transfer exceeds $\sim 10^9$ s^{-1}, a single average-valence quadrupole-split doublet is observed.

^{57}Fe Mössbauer data for a sample consisting of parallelepiped crystals of **1** were collected at temperatures ranging from 25 to 300 K. Selected spectra are shown in Figure 5, and the complete set of fitting parameters are listed in Table V. At temperatures above 100 K, the spectrum of this sample shows a single quadrupole-split doublet which is characteristic of valence-detrapped cation in which the intracation electron-transfer rate exceeds $\sim 10^9$ s^{-1}. However, the 25 K spectrum shows a superposition of valence-trapped and valence-detrapped signals. Upon decreasing the temperature of the sample to 25 K, domains form in which electron transfer is slower than $\sim 10^6$ s^{-1}. These valence-trapped domains presumably nucleate and grow around defect sites in the crystals. To test this assumption, we mechanically ground (~ 5 min in a mortar and pestle) a collection of the parallelepiped crystals purposely intending to introduce a higher concentration of defect sites. The ^{57}Fe Mössbauer spectrum of this sample at various temperatures is shown in Figure 6, and the fitting parameters are collected in Table VI. An amazing change in the spectrum occurs as a result of grinding the sample. While the spectrum of the nonground parallelepiped needle crystals of **1** at 110 K shows only one doublet (valence detrapped), the spectrum of the ground crystallites is a superposition of valence-trapped and -detrapped signals. As the temperature of the ground sample is increased, the intensity of the detrapped signal grows at the

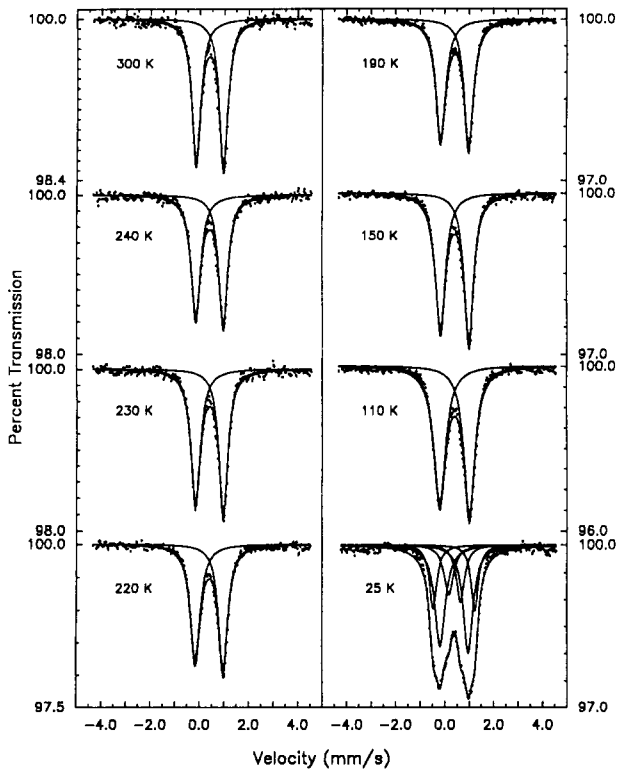

Figure 5. Variable-temperature ^{57}Fe Mössbauer spectrum for a sample of 1′,1‴-dibenzylbiferrocenium triiodide (**1**) consisting of a collection of parallelepiped (needle) crystallites.

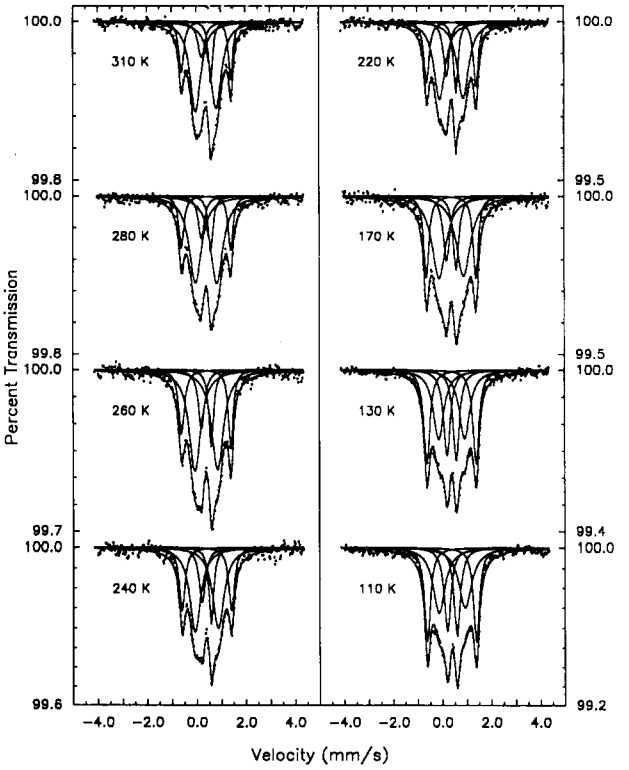

Figure 6. Variable-temperature ^{57}Fe Mössbauer spectrum for a ground sample of parallelepiped crystallites of 1′,1‴-dibenzylbiferrocenium triiodide (**1**).

expense of the trapped signal. Nevertheless, even at 310 K some of the trapped valence signal persists. It should be noted that microanalytical data for the ground sample were found to be identical with those of the unaltered portion of the sample.

Mechanical grinding is known to increase the number of defects in a crystalline lattice. When the parallelepiped crystals of **1** are ground, the number of defect sites undoubtedly increases. A

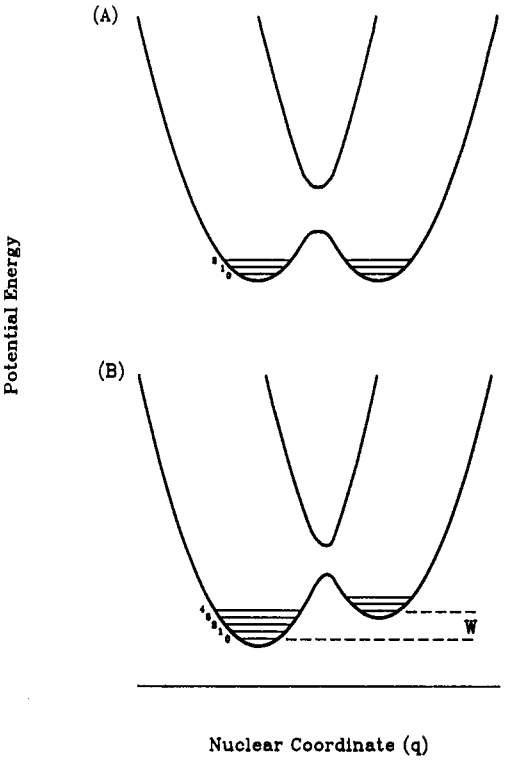

Figure 7. Potential energy plotted as a function of the out-of-phase combination of the two symmetric metal–ligand breathing vibrational modes on the two halves of a binuclear mixed-valence species. Diagram A is for the symmetric mixed-valence complex in the absence of environmental effects. Diagram B results if the environment about the binuclear mixed-valence complex is asymmetric. Vibrational levels are indicated.

1′,1‴-dibenzylbiferrocenium cation which is situated close to a defect such as a dislocation would become trapped due to the introduction of a zero-point energy difference between the two vibronic descriptions of the cation (Figure 7). This zero-point energy difference is caused by the perturbations from the nearby lattice abnormality. For mixed-valence cations on the fringe of the distortion's influence, the zero-point energy difference is less pronounced. With increasing temperature these cations on the fringe of the defect develop enough thermal energy to populate a vibrational level from which they can tunnel to the other vibronic state. Then, electron transfer occurs at an appreciable rate. However, for cations nearer to the distortion, the zero-point energy difference is much larger than kT even at 300 K, and consequently electron transfer in these cations remains slow. This accounts for the increase in the detrapped signal spectral area with increasing temperature as well as the persistence of the trapped valence signal above 300 K. That is, there is a distribution in environments about the mixed-valence cations which leads to a distribution in zero-point energy differences (W in Figure 7).

The differences in the ^{57}Fe Mössbauer spectral properties of the two polymorphs of **1** (triclinic and monoclinic) are attributable to differences in the crystalline environment surrounding the mixed valence 1′,1‴-dibenzylbiferrocenium cations. In the $P\bar{1}$ polymorph, the crystal structure results show that the time averaged environment of the cation is symmetric with respect to the two iron ions of a single cation. Rapid electron transfer is then possible in this symmetric arrangement. The asymmetric environment of the mixed-valence cations in the $P2_1/n$ polymorph energetically favors one valence description over the other and as a consequence slow electron-transfer results. Hence, the environment surrounding the mixed-valence cation plays an important if not dominating role in determining the electron-transfer rate in the mixed-valence 1′,1‴-dibenzylbiferrocenium cation of **1**.

Electron Paramagnetic Resonance. At low temperatures, the EPR spectra of mixed-valence biferrocenium salts consist of an axial or nearly axial ($g_x = g_y$) rhombic signal.[10,15,21] The g-tensor

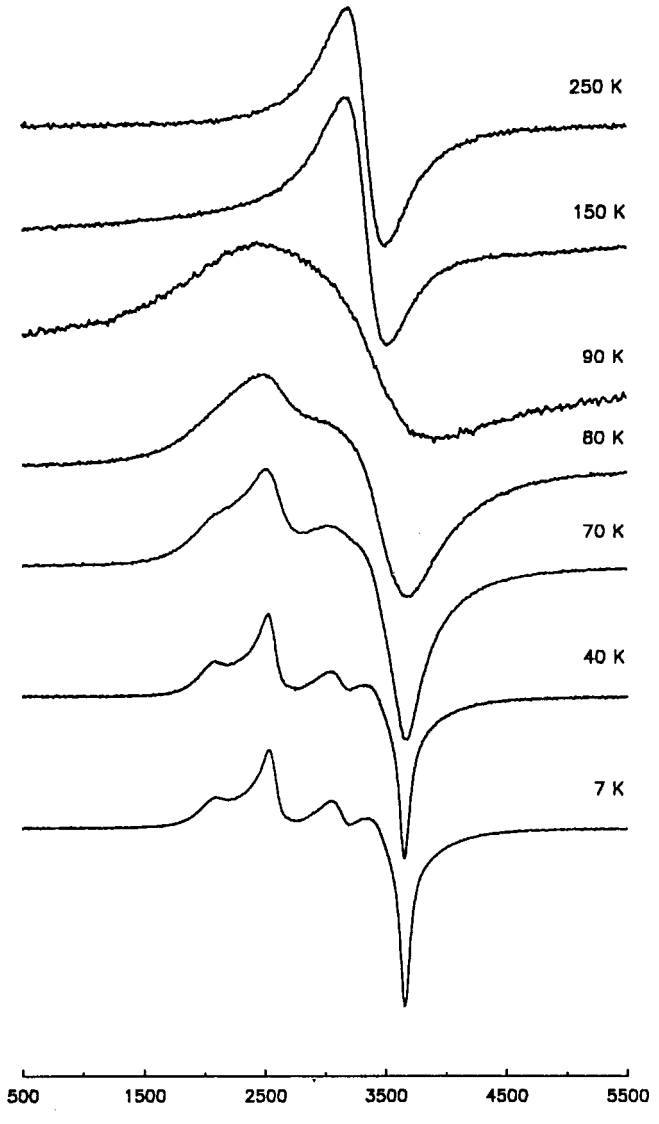

Figure 8. Temperature dependence of X-band EPR spectrum of a recrystallized sample of 1',1'''-dibenzylbiferrocenium triiodide (**1**).

anisotropy ($\Delta g = g_{\parallel} - g_{\perp}$) for disubstituted biferrocenium salts varies considerably, and this anisotropy can be used as a rough estimate of the nature of the electronic ground state of a mixed-valence biferrocenium cation.[22] A small g-tensor anisotropy ($\Delta g < 0.7$) indicates a mixed-valence moiety which has little or no barrier to electron transfer and essentially a valence delocalized electronic ground state. Larger anisotropy in the g-tensor has been associated with valence localized structures. An empirical correlation has been observed between the g-tensor anisotropy and the ^{57}Fe Mössbauer spectral properties of a number of binuclear ferrocene systems.[10,15,22] Generally, systems with larger g-tensor anisotropy ($\Delta g > 1.5$) are valence trapped on the Mössbauer time scale at all temperatures, while those with small anisotropy ($g <$ 1.1) are valence detrapped through out the thermally accessible temperature range. Systems with Δg between 1.1 and 1.5 show Mössbauer behavior intermediate between these two extremes; they are valence trapped at low temperatures and can become detrapped at higher temperatures.

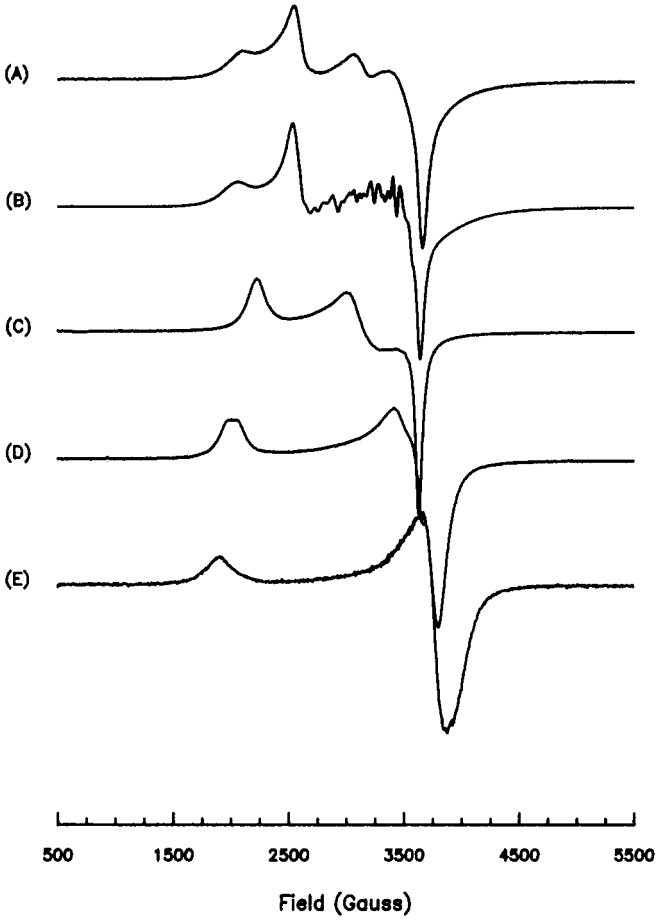

Figure 9. X-band EPR spectra for various polycrystalline samples of 1',1'''-dibenzylbiferrocenium triiodide at 7 K: (A) sample of **1** recrystallized from 1:1 dichloromethane/hexane solution, (B) initial unrecrystallized sample of **1**, (C) and (D) two other unrecrystallized samples of **1**, and (E) ethanol glass of **1**.

X-band EPR spectra were run for the recrystallized sample of 1',1'''-dibenzylbiferrocenium triiodide, **1**, at various temperatures and are shown in Figure 8. The 7 K spectrum of **1** is clearly a superposition of three distinct signals: two axial $S = 1/2$ powder patterns and an isotropic $g = 2.16$ feature. The feature at $g_{\parallel} = 3.23$ is the $g_{\parallel}$ edge of an axial pattern where the $g_{\perp}$ feature occurs $\sim$1.94. The g-tensor anisotropy of this signal is $\Delta g = 1.29$ and is typical of that observed for other 1',1'''-dibenzylbiferrocenium salts.[9a] This anisotropy falls in the intermediate region of the empirical correlation discussed above and therefore is consistent with Mössbauer behavior of the plate-like $P2_1/n$ polymorph of **1**.

The second $g_{\parallel}$ feature occurs at $g = 2.66$ and is evidently the $g_{\parallel}$ edge of another axial pattern where the $g_{\perp}$ signal is at $g \sim$ 1.90. The g-tensor anisotropy of this axial signal is considerably reduced ($\Delta g = 0.76$) from the first case; it is expected that the ^{57}Fe Mössbauer spectrum for this species would indicate a valence-detrapped species at all temperatures. This second axial EPR signal undoubtedly arises from the mixed-valence cations in the $P\bar{1}$ polymorph of **1**.

The third EPR signal observed in the 7 K spectrum of **1** is an isotropic $g \simeq 2.16$ feature, and this is the only one present at temperatures above 150 K for a polycrystalline sample (Figure 8). One possible origin for this isotropic signal arises from intercation spin exchange[23] resulting from a weak intercation magnetic exchange interaction which develops between valence-detrapped cations at high temperatures. Some experimental evidence that supports the view that it is a process characteristic

(20) (a) Nakashima, S.; Sano, H. *Bull. Chem. Soc. Jpn.* **1989**, *62*, 3012. (b) Nakashima, S.; Katada, M.; Motoyama, I.; Sano, H. *Bull. Chem. Soc. Jpn.* **1986**, *59*, 2923. (c) Ijima, S.; Saida, R.; Motoyama, I.; Sano, H. *Bull. Chem. Soc. Jpn.* **1981**, *54*, 1375.

(21) (a) Nakashima, S.; Masuda, Y.; Motoyama, I.; Sano, H. *Bull. Chem. Soc. Jpn.* **1987**, *60*, 1673. (b) Nakashima, S.; Masuda, Y.; Motoyama, I.; Sano, H. *Hyperfine Inter.* **1988**, *40*, 319.

(22) Kramer, J. A.; Hendrickson, D. N. *Inorg. Chem.* **1980**, *19*, 3330.

(23) Molin, Y. N.; Salikhov, K. M.; Zamaraev, K. I. *Spin Exchange, Principles and Applications in Chemistry and Biology*; Springer-Verlag: Berlin, 1980.

of interactions between paramagnetic molecules can be given. The X-band EPR spectrum of **1** in a frozen ethanol glass is available in the supplementary material. The 7 K spectrum consists of a typical axial pattern ($g_\parallel = 3.56$, $g_\perp = 1.74$, and $\Delta g = 1.82$) with no $g \simeq 2$ feature. As the temperature is increased, this axial signal broadens and becomes unobservable above 77 K with no appearance of a $g \simeq 2$ signal. Consequently, this indicates that the $g \simeq 2.16$ signal seen for the polycrystalline sample is likely the result of intermolecular interactions in the magnetically concentrated conditions of a crystalline lattice. It is unlikely that the $g \simeq 2.16$ signal represents cations which are electronically delocalized for several reasons. First, the IR spectrum of electronically delocalized species show a single C-H bending vibration midway between that of an Fe^{II} and Fe^{III} metallocenes. Two C-H bending bands, one characteristic of Fe^{II} and the other Fe^{III}, are seen in the IR spectrum of **1**.[10] Second, an electronically delocalized species still shows some residual g-tensor anisotropy.[24]

X-band EPR spectra collected on different microcrystalline samples of **1** serve to illustrate further the extreme "environmental" sensitivity that this mixed-valence complex exhibits. The spectrum at 7 K of four different polycrystalline samples together with that for the ethanol glass sample are shown in Figure 9. All of these spectra are the superposition of a number of signals. The exact position of the $g_\parallel$ features for the various polycrystalline samples varies appreciably from one sample to another. All of these polycrystalline samples exhibit only the $g \simeq 2$ signal when the temperature is increased.

Concluding Comments. The polymorphism discovered for 1′,1‴-dibenzylbiferrocenium triiodide definitively shows that the immediate environment of the mixed-valence cation plays an important role in determining the rate of intramolecular electron transfer. In the $P\bar{1}$ polymorph of **1** the electron-transfer rate is faster than 10^9 s^{-1} above ~25 K, while in the $P2_1/n$ polymorph the rate is slower than 10^6 s^{-1} for all temperatures. The only differences between the cations in these salts are attributable to their environment. The most extreme environmental control of the rate of intramolecular electron transfer is seen by mildly grinding the $P\bar{1}$ polymorph of complex **1**. The original sample is valence detrapped down to ~25 K. Grinding leads to a portion of the polycrystalline solid to remain trapped up to 310 K. This is a surprising result in view of the fact that the powder X-ray diffraction data show that there is no change in space group upon grinding. The environment can turn on or off the electron transfer.

Acknowledgment. We are grateful for funding from the National Institutes of Health Grant HL13652 (D.N.H.). Research at the University of Colorado was supported by the National Science Foundation under Grant CHE 88-09923 (C.G.P.).

Supplementary Material Available: Complete tables of positional parameters, bond lengths and angles, and thermal parameters for the $P\bar{1}$ form of complex **1** at 298 and 135 K, table of Mössbauer parameters for a ground sample of the $P\bar{1}$ polymorph of complex **1**, tables of positional parameters, thermal parameters, and bond lengths and angles for the $P2_1/n$ polymorph of complex **1** at 296 K, and figures showing powder X-ray patterns, temperature dependence of the X-band EPR spectrum of the frozen ethanol glass of complex **1**, and a packing diagram of the $P2_1/n$ polymorph of complex **1** (17 pages); tables of observed and calculated structure factors for the $P\bar{1}$ form of complex **1** at 298 and 135 K and the $P2_1/n$ polymorph of complex **1** at 296 K (88 pages). Ordering information is given on any current masthead page.

(24) LeVande, C.; Bechgaard, K.; Cowan, D. O.; Mueller-Westerhoff, U. T.; Eilbracht, P.; Candela, G. A.; Collins, R. L. *J. Am. Chem. Soc.* **1976**, *98*, 3181.

Selective Two-Component Self-Diffusion Measurement of Adsorbed Molecules by Pulsed Field Gradient Fourier Transform NMR

Uwe Hong, Jörg Kärger,* and Harry Pfeifer

Contribution from the Sektion Physik, Universität Leipzig, Linnéstrasse 5, 7010 Leipzig, Germany. *Received September 7, 1990*

Abstract: The two-component self-diffusion of C_2H_4 and C_2H_6 adsorbed in NaX zeolite crystals has been measured by ^1H pulsed field gradient (PFG) Fourier transform NMR. The results so obtained are compared with single-component self-diffusion measurements and with values for the intracrystalline mean residence times, determined by means of NMR tracer desorption experiments.

Application of the PFG NMR method[1] to diffusion studies in zeolitic adsorbate-adsorbent systems[2,3] has substantially contributed to a deeper understanding of molecular migration in the interior of zeolite crystallites.[4,5] This development was in particular stimulated by the ability of PFG NMR to monitor directly the intracrystalline molecular displacements. As a substantial advantage in comparison to the traditional way of studying intracrystalline diffusion by following the rate of molecular uptake, this peculiarity of PFG NMR implies the possibility of determining the diffusivities of individual components within a multicomponent system. Since during their technical application zeolites will be generally used under the conditions of multicomponent adsorption,[5] the significance of selective diffusion studies is obvious.

The traditional way of performing such experiments is to use perdeuterated compounds or compounds without any hydrogen so that only one of the various compounds yields the ^1H NMR signal[2] from which the diffusivity may be easily determined. Unfortunately, this way of selective diffusion measurement necessitates additional experimental preparation, since for the study of a system containing n components at least n various NMR samples must be prepared, each of them with a different compound in the hydrogen form.

A more straightforward possibility of selective self-diffusion measurements is provided by Fourier transform NMR. In this method the total NMR signal is split up in separate signals of

(1) Stejskal, E. O.; Tanner, J. E. *J. Chem. Phys.* **1965**, *42*, 288.
(2) Kärger, J.; Pfeifer, H. *Zeolites* **1987**, *7*, 90.
(3) Förste, C.; Kärger, J.; Pfeifer, H. *J. Am. Chem. Soc.* **1990**, *112*, 7.
(4) Barrer, R. M. *Zeolites and Clay Minerals as Sorbents and Molecular Sieves*; Academic Press: London, 1978.
(5) Ruthen, D. M. *Principles of Adsorption and Adsorption Processes*; John Willey; New York, 1984.

0002-7863/91/1513-4812$02.50/0